Electrical Conductivity, Near-Infrared Absorption, and Thermal Lens Spectroscopic Studies of Percolation of Microemulsions

Mauricio S. Baptista and Chieu D. Tran*

Department of Chemistry, Marquette University, P.O. Box 1881, Milwaukee, Wisconsin 53201-1881

Received: December 17, 1996; In Final Form: March 5, 1997[⊗]

Microemulsions of negatively charged (sodium bis(2-ethylhexyl)sulfosuccinate, AOT) and positively charged (dodecylmethylbutylammonium bromide and benzyldimethylhexadecylammonium chloride) surfactants were studied below and above the percolation thresholds by electrical conductivity, near-infrared absorption, and thermal lens spectrometry. It was found that the AOT microemulsions undergo percolation at a relatively high concentration (about 27% of water (v:v)) and show no variation in the thermal lens effect (θ/AP_0) as a function of water concentration. These results seem to indicate that the AOT microemulsions consist of small reversed micelles, and this structure is the same below and above the percolation threshold. Conversely, for microemulsions prepared with positively charged surfactants, the percolation occurs at relatively low concentration (around 10% of water (v:v)), and also it is in this region that the thermal lens effect (i.e., θ/AP_0) as a function of water undergoes changes. It seems that the structure of these positive microemulsions changes concomitantly with the percolation. Specifically, these positive microemulsions form larger interconnected aggregates or bicontinuous structures in solution above percolation threshold concentration.

Microemulsions are thermodynamically stable isotropic mixtures of oil, water, and surfactant. They have been extensively studied using various techniques such as spin-echo NMR, fluorescence quenching, neutron and light scattering, and electrical conductivity.[1,2] However, in spite of these numerous studies, internal structures of some microemulsions are still not fully understood.

Electrical conductivity measurements have been used to provide information on the continuity of the aqueous phase. For some microemulsions, a small change in one of the system variables (e.g., the ratio of [water] to [surfactant] (W_0 = [water]/[surfactant]), the concentration of the micellar phase or the temperature) leads to a significant change in the electrical conductivity. This phenomenon has been called percolation.[3] Exact molecular mechanisms of the percolation phenomena are still a subject of much debate in the literature. For instance, ion hopping between micelles has been suggested as the cause for these phenomena.[4] Fast material and water exchange when micelles coalesce may also be responsible for these.[5,6] Another possibility is the formation of bicontinuous structures in solution.[7−11] Bicontinuous structures are understood as having a dynamic nature where both water and oil are continuous phases and are separated by a small curvature surfactant film. The formation of random and momentary continuous water channels would therefore explain the large increase in electrical conductivity.[7−12]

Clearly, electrical conductivity measurements do not provide sufficient evidence to unambiguously characterize the structures of the microemulsions.[12,13] It is important, therefore, to develop new methods that can provide structural information of microemulsions. In this work the structure of microemulsions was investigated by using the near-IR absorption and thermal lens techniques together with the electrical conductivity. It will be shown that near-IR absorption and thermal lens measurements can provide complemental information necessary to arrive to a conclusion of the internal structure of the microemulsions. Such information can be obtained because absorption in the near-IR region (750 to around 2600 nm)[14] is due to the overtone and/or combination of transitions of the C−H, O−H, and N−H groups. Any compound that has C−H, O−H, or N−H groups in its structure will have absorption in this region.[14−16] On the other hand, the thermal lens technique is based on the measurement of the nonuniform heating generated in the sample as a result of the laser excitation. This nonuniform heating will generate a refractive index gradient that acts as a thermal lens which is monitored by a probe laser. When the absorbing species reach the thermal lens steady-state condition (i.e., the rate of heat generated equals the rate of heat conducted out), the relative change in the beam center intensity in the far field, $\Delta I_{bc}/I_{bc}$, is given by[16−18]

$$\frac{\Delta I_{bc}}{I_{bc}} = \frac{1.206 P_0 A(-\mathrm{d}n/\mathrm{d}T)}{\lambda k} \qquad (1)$$

where P_0 is the power of the excitation laser, λ is probe-laser wavelength, A is sample absorbance, and $\mathrm{d}n/\mathrm{d}T$ and k are the temperature coefficient of refractive index and the thermal conductivity of the medium, respectively.

It is evident that changes in the thermooptical properties (k, $\mathrm{d}n/\mathrm{d}T$) of the medium will cause changes in the thermal lens signals. It is expected, therefore, that changes in the structure of the sample that induce changes in the thermooptical properties of the medium could be probed by this technique.[19,20] In fact, the thermal lens technique has been successfully used to study the effect of nonelectrolytes and surfactants on the structure of water.[19] In this study, the thermal lens signal was measured as a function of the temperature of the system and the concentration of solute.[19]

Variables, such as W_0, temperature, and concentration of micellar phase, can lead to changes in the structures of the microemulsions.[1,2] Rather than changing all of these variables, in this study, only the effect of the concentration of the micellar phase at relatively low W_0 values (W_0 = 15 or 16) was investigated. Under these conditions at the region where oil is in excess, the structure of the microemulsion is constituted of small reversed micelles.[1,2] By studying the microemulsion properties at these low W_0 values as a function of the micellar

[⊗] Abstract published in *Advance ACS Abstracts,* May 1, 1997.

S1089-5647(97)00017-5 CCC: $14.00

phase concentration, it may be possible to determine the preference of different surfactant films to form either low- or high-curvature structures in solution.

Several microemulsion systems prepared from positively and negatively charged surfactants with different oil phases were investigated. It will be shown that by measuring the thermal lens signal as a function of the concentration of dispersed phase, below and above the percolation threshold, it was possible to characterize which systems and at which micellar phase concentrations micelles undergo changes in the internal structure. Knowledge on the internal structure of the microemulsions may be obtained from this information together with those gained from the electrical conductivity measurements. It will be demonstrated that the microemulsions prepared with the negatively charged surfactant, sodium bis(2-ethylhexyl) sulfosuccinate (AOT), are constituted of globular reversed micelles of similar size below and above the percolation threshold. Interestingly, in the case of the microemulsions prepared with the positively charged surfactants, dodecyldimethylbutylammonium bromide (DDBABr) and benzyldimethyl-*n*-hexadecylammonium chloride (BDHAC1), the reversed micelles in solution will grow and will form interconnected aggregates concomitantly with the increase in the concentration of dispersed phase. This will eventually lead to the development of bicontinuous structures in solution.

Experimental Section

Materials. Water was deionized and distilled. Its electrical conductivity (σ) was measured to be 2 μS/cm. 1,2,2-Trichorotrifluoroethane was purchased from Pfaltz & Bauer. Hexane was distilled over sodium. Benzene (Fisher Scientific, ACS spectranalyzed) was distilled prior to use. The purity of chlorobenzene (Fisher Scientific) was verified by NMR. Sodium bis(2-ethylhexyl) sulfosuccinate (AOT) was purified with activated charcoal and dried for 2 days under vacuum at 90 °C. Dodecyldimethylbutylammonium bromide (DDBABr) was synthesized using *N*,*N*-dimethyldodecylamine (Aldrich, 97%) and 1-bromobutane (TCI). The compound was recrystallized six times with acetyl acetate and dried for 2 days under vacuum at 90 °C. The NMR spectra of DDBABr indicate that the product is free of impurities, including water and reactants. Benzyldimethyl-*n*-hexadecylammonium chloride (BDHAC1) was purchased from Eastman Kodak and dried for 2 days under vacuum (90 °C) prior to use.

Methods. The absorption spectra were measured in the Shimadzu UV−vis spectrophotometer (UV-1201), using a 1 cm quartz cuvette. The absorption spectra shown in this work were corrected for the increase in the scattered light concomitant with the increase in the concentration of the dispersed phase. This correction was performed by subtracting the amount of the scattered light measured at 800 nm (a wavelength at which no absorption was detected for any of the samples investigated). These corrections were performed because it was necessary to normalize the thermal lens signals for different absorbances of each sample. The thermal lens signal is proportional to the light absorbed by the sample, which does not include the scattered light. The amount of light scattered by the samples used in the thermal lens experiments (2 mm quartz cells) was determined to be equal or less than 0.5% and to be constant in the wavelength region utilized. Thorne and Bobbitt[21] performed absorption measurements by the thermal lens and normal transmission techniques for samples that have much higher scattering background than the samples used in this study. They concluded that the absorption measured with the thermal lens technique is proportional only to the amount of light absorbed and therefore is immune to the increased scattering background in the samples. This further confirms the validity of the correction performed.[21]

The electrical conductivity measurements were performed in a Hanna instrument (HI 8333). It operates at 1 kHz and has a cell constant of 1 cm^{-1}. The accuracy of the instrument was tested using a calibration standard from Fisher that had 9869 μS/cm ± 0.25%.

The thermal lens decays were generated using the same instrumentation and were treated using the same methodology as previously described.[16,19] Basically, a titanium−sapphire laser is used to provide the excitation beam in the near-IR region. The heat generated in the sample as a consequence of absorption of the near-IR radiation is detected by a He−Ne laser. The time dependence of the probe beam center intensity *I(t)* is detected by a photodiode in the far field. *I(t)* can be satisfactorily described by[22−25]

$$I(t) = I(0)\left[1 - \theta \arctan\left[\frac{2\xi}{3 + \xi^2 + (9 + \xi^2)t_c/2t}\right] + \left\{\frac{\theta}{2}\arctan\left[\frac{2\xi}{3 + \xi^2 + (9 + \xi^2)t_c/2t}\right]\right\}^2 + \left(\frac{\theta}{4}\ln\left\{\frac{[(2 + t_c/t)(3 + \xi^2) + 6t_c/t]^2 + 16\xi^2}{(9 + \xi^2)^2(2 + t_c/t)^2}\right\}\right)^2\right] \quad (2)$$

where ξ is related to the distance between the sample and the beam waist Z_1, and the confocal distance, Z_c, by

$$\xi = Z_1/Z_c \quad (3)$$

The parameter θ is related to the laser wavelength (λ), laser power (P_0), the sample absorbance (A), the temperature coefficient of the refractive index (dn/dT), and the thermal conductivity k of the solvent by eq 4:

$$\theta = [2.303P_0A(-dn/dT)]/\lambda k \quad (4)$$

The thermal time constant t_c is given by

$$t_c = \omega^2\rho c_p/4k \quad (5)$$

where c_p is the heat capacity, ρ is the density, and ω is the $1/e^2$ radius of the pump beam with a Gaussian profile.

From the recorded time dependence of the beam center intensity (*I(t)*), θ, which is related to the thermal lens strength, and the thermal time constant t_c can be obtained by curve fitting of the experimental data according to eq 2. θ and t_c for several microemulsion systems were measured as a function of the micellar phase concentration. The value of θ was corrected for sample absorption and laser excitation power. The calculated θ/AP_0 is, therefore, proportional to k and dn/dT. All thermal lens signals were measured in 2 mm quartz cuvettes.

The microemulsions were prepared with high concentration of dispersed phase and then diluted using the oil phase, keeping the value of [water]/[surfactant] ratio (W_0) constant. All the experimental data shown are plotted as a function of water concentration measured in percentage (v:v). Because W_0 was kept constant, water percentage is proportional to the total concentration of the micellar phase. All the experiments reported were measured at 21.5 ± 0.1 °C.

Results

Three different surfactants, sodium bis(2-ethylhexyl) sulfosuccinate (AOT), dodecyldimethylbutylammonium bromide

TABLE 1: Examples of Reported Microemulsion Systems

microemulsion system	Φ^a	W_0	exptl techniques and refs
AOT/hexane water	0.2−0.6	0−50	electrical conductivity[26]
AOT/isooctane/water	0.2−0.6	0−50	electrical conductivity[26]
AOT/*n*-heptane/water	0.1−0.8	2−40	FT-IR,[27a] calorimetry,[27b] refractive index[27c]
AOT/*n*-heptane/water	0.1−0.7	0−40	density, sound velocity, electrical conductivity, viscosity, adiabatic compressibility[28]
AOT/decane/D_2O	0.59−0.71	15−39	small-angle neutron scattering[29]
AOT/decane/D_2O	0.35−0.75	40.8	quasi-elastic light scattering
BDHACl/benzene/water	0.0−0.2	7−33	electrical conductivity, light scattering, self-diffusion fluorescence[31]
BDHACl/benzene/water	0.0−0.35	0−80	light scattering, time-resolved fluorescence, electrical conductivity, self-diffusion ^{1}H NMR[32,33]
DDBABr/Cl−benzene/water	0.0−0.35	0−60	

[a] Φ is the dispersed phase volume fraction.

SCHEME 1: Structures and Abbreviations of Surfactants Used in This Study

AOT - sodium bis(2ethylhexyl)sulfosuccinate

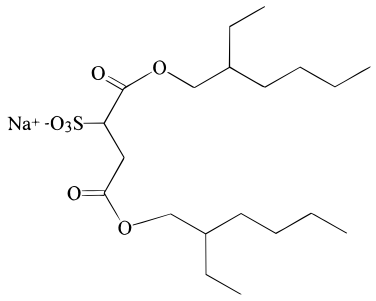

DDBABr - Dodecyldimethylbutylammonium bromide

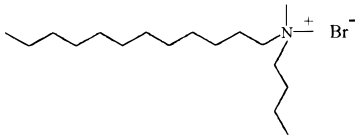

BDHACl- benzyldimethyl-n-hexadecylammonium chloride

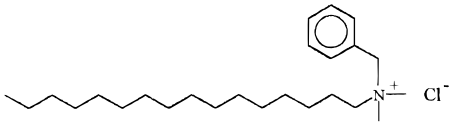

(DDBABr), and benzyldimethyl-*n*-hexadecylammonium chloride (BDHACl), were used in this study. Their structures are shown in Scheme 1. As illustrated, the first is anionic while the other two are cationic surfactants having relatively similar structure except that BDHACl has a phenyl group. These surfactants were selected in order to gain insight into effects of charges and phenyl moiety on percolation. Furthermore, they are known to form transparent, single phase, isotropic w/o microemulsions. Some of reported studies using these surfactants are tabulated in Table 1 together with techniques previously used to study them. In this study, trichlorotrifluoroethane was used as the solvent in the first set of experiments because this solvent has no C−H group and, hence, is transparent is the near-IR region. It is interesting to observe that similar to other solvents listed in Table 1 (e.g., hexane, isooctane, heptane, decane, and benzene) AOT, BDHACl, and DDBABr form stable, transparent, single phase, isotropic microemulsions in $CF_2ClCFCl_2$ whereas no stable microemulsions were observed for these surfactants in carbon tetrachloride in the concentration range used in this study.

Shown in Figure 1A is the electrical conductivity of AOT/$CF_2ClCFCl_2$/water microemulsion, measured as a function of the water concentration. It is evident that close to 27% water the electrical conductivity starts to increase. At 32% the electrical conductivity is more than 3 orders of magnitude higher than it was at 25%. This behavior is characteristic of percolation. It should be noted that the microemulsion percolates only at a very high concentration of the dispersed phase. The weight percentage of the dispersed phase [ϕ_D = (water + surfactant)/(total)] at 27% of water is equal to 59%.

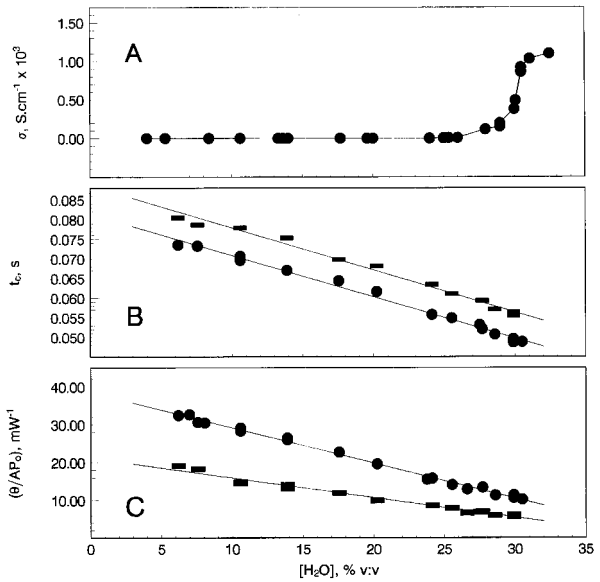

Figure 1. (A) Electrical conductivity, (B) t_c at 975 (●) and 910 nm (■), and (C) θ/AP_0 at 975 (●) and 910 nm (■) as a function of water percentage for the AOT/$CF_2ClCFCl_2$/water microemulsions ([AOT] = 1.12 M at 30.44% water).

The near-IR spectra of the microemulsions with different water concentrations (which is proportional to the concentration of the dispersed phase) are shown in Figure 2. As illustrated, increasing the concentration of micellar phase at a constant W_0 value of 15 led to an increase in the absorbance in the whole wavelength region. The absorption peak at 975 nm is due to a combination transitions ($2\nu_2 + \nu_3$) of the O−H group of water.[16,32] The shoulder at 910 nm is due to the second C−H overtone of the surfactant.[16,32] Accordingly, the thermal lens signals were measured at 975 and 910 nm in order to monitor the aqueous phase and the surfactant film of the microemulsion. As stated earlier, the organic phase in this case is $CF_2ClCFCl_2$, which has no absorption in this near-IR region.

Figure 1B shows the values of thermal lens time constant (t_c) measured as a function of the water percentage at 975 and 910 nm. Increase in the concentration of the dispersed phase leads to a decrease in the t_c value for both wavelengths. As evident from eq 5, the t_c value depends on several parameters that may change as a function of the concentration of the dispersed phase (k, ρ, c_p). While all these parameters may contribute to the observed variation in t_c, it is expected that the variation of the thermal conductivity (k) is the dominant effect. As listed in Table 2, the thermal conductivity of the organic phase ($CF_2ClCFCl_2$) is much smaller than that of water.

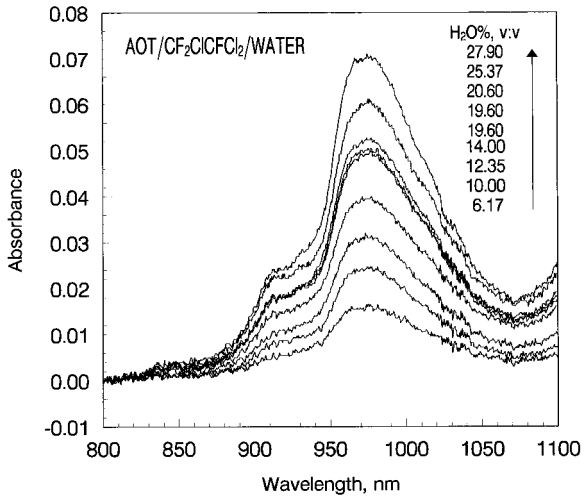

Figure 2. Near-IR absorption spectra of the AOT/$CF_2ClCFCl_2$/water microemulsions with different water concentrations ([AOT] = 1.03 M at 27.90% water).

TABLE 2: Thermooptical Properties of the Solvents Used in This Work

solvent	k, W cm^{-1} K^{-1} × 10^3	$-$dn/dT, K^{-1} × 10^4
H_2O	6.1[a]	0.90[a]
benzene	1.37[b]	6.52[b]
Cl−benzene[c]	1.20 ± 0.01	5.4 ± 0.4
hexane	1.23[b]	5.2[b]
$CClF_2CCl_2F$	0.66[d]	4.5[d]

[a] From ref 20. [b] From ref 35. [c] This work. [d] From ref 36.

Therefore, when the concentration of $CF_2ClCFCl_2$ is increased (percentage of water is decreased), it is expected that t_c would increase (see eq 5). This, in fact, was observed experimentally.

Figure 1C shows the parameter θ/AP_0 as a function of water concentration. Similar to the effect observed for t_c, there is a decrease in the θ/AP_0 value concomitant with the increase in the concentration of the dispersed phase at both wavelengths, 910 and 975 nm. This effect can be explained based on the relatively larger dn/dT value and the smaller k value of $CF_2ClCFCl_2$ compared to those of water (Table 2). It is, therefore, expected that increasing the concentration of the organic phase would lead to an increase in dn/dT (and decrease in k) of the microemulsion. Consequently, θ/AP_0 would increase (see eq 4). This was, in fact, observed experimentally.

It is clear from Figure 2B that t_c at a specific water concentration measured at 975 nm is not the same as the t_c measured at 910 nm. The same effect was also observed for θ/AP_0. This is probably due to differences in the beam-waist spot size (ω) at these two wavelengths. Unfortunately, it is difficult to experimentally determine ω accurately.[20] This effect could be further clarified by calculating k and dn/dT of the microemulsions. However, because of the lack of experimental values of c_p for this specific microemulsion, it is not possible to accurately calculate k and dn/dT values. Although the values of c_p could be roughly estimated from the literature values of the microemulsion components, it is known that c_p in the case of microemulsions is very sensitive to changes in the topology of the surfactant interfaces. In fact, c_p exhibit nonlinear variations as a function of temperature, W_0, or dispersed phase concentration.[11,35−37]

It is important to point out that the θ/AP_0 values measured above the percolation threshold fell into the same straight line as the values measured below the percolation threshold for both wavelengths. The slope of the curve "θ/AP_0 versus water concentration" at 975 nm, calculated using all the experimental

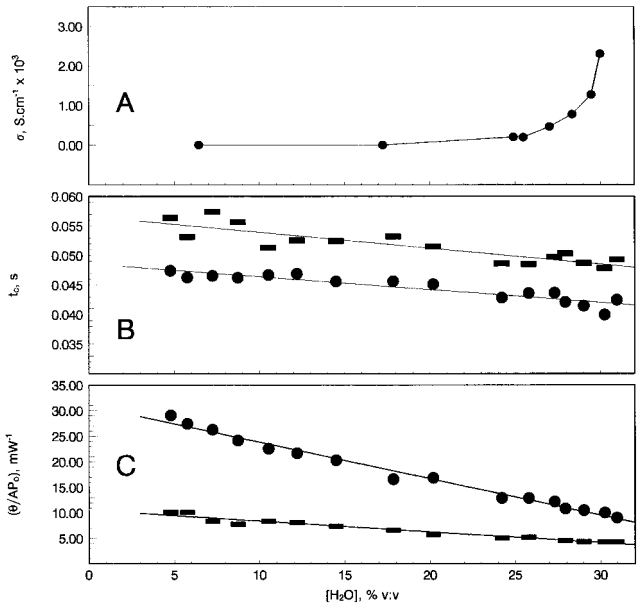

Figure 3. (A) Electrical conductivity, (B) t_c at 975 (●) and 910 nm (■), and (C) θ/AP_0 at 975 (●) and 910 nm (■) as a function of water percentage for the AOT/hexane/water microemulsions ([AOT] = 1.14 M at 30.95% water).

points, was 0.93 ± 0.02 mW^{-1} %$^{-1}$. The slope calculated from samples which have water concentrations higher than 27.5% (i.e., 27.5−31% of water) was 1.0 ± 0.26 mW^{-1} %$^{-1}$. The slope calculated from samples with water concentrations lower than 27.5% (27.5−6%) was 0.94 ± 0.02 mW^{-1} %$^{-1}$. It is evident that these slopes are the same within experimental errors. It is noteworthy to add that the electrical conductivity measurements indicate that this microemulsion undergoes percolation at water concentrations above 27.5%. Therefore, it is evident that θ/AP_0 remains the same at either below or above the percolation.

Another microemulsion was prepared using hexane instead of $CF_2ClCFCl_2$. Figure 3A shows the electrical conductivity as a function of water concentration (v:v) for the AOT/hexane/water microemulsion, at a constant W_0 of 15. As illustrated, the electrical conductivity starts to increase only at a high dispersed phase concentration (above 26% water). This is similar to the effect observed for the microemulsion prepared with $CF_2ClCFCl_2$. Again at 31% water the electrical conductivity is more than 3 orders of magnitude higher than it was at 25%.

Shown in Figure 4 are the near-IR spectra of these microemulsions at different concentrations of micellar phase. As depicted, with the increase in the concentration of the micellar phase at constant W_0 value, there is an increase in the absorbance in the 830−1100 nm region. The transition with maximum at 975 nm is due to the O−H group of water.[32] The band whose peak is at 900−910 nm is the overtone transition of the C−H groups in hexane and AOT.[32] Accordingly, the thermal lens signals were measured at 975 and 910 nm.

Figure 3B shows the variation of t_c as a function of water concentration at 975 and 910 nm. The increase in t_c with the decrease in the concentration of the dispersed phase may again be explained based on the smaller k value of hexane compared with k of water (Table 1). An increase is also observed for θ/AP_0 at both 975 and 910 nm (Figure 3C). This effect is similar to that observed for the microemulsions prepared with $CF_2ClCFCl_2$. It is probably related to the differences in the thermooptical properties between water and hexane (see Table 2). It can be noted that the θ/AP_0 value measured above the

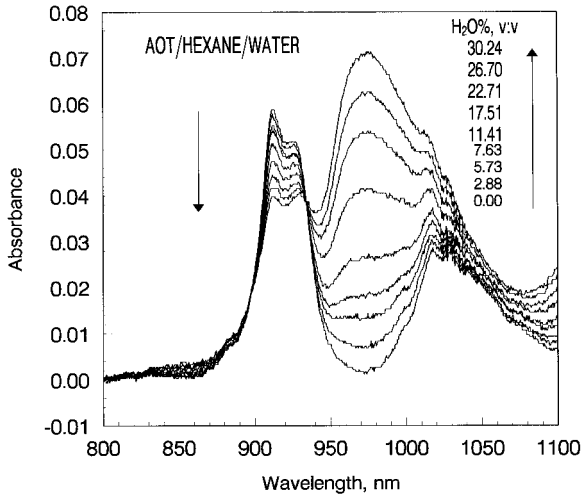

Figure 4. Near-IR absorption spectra of the AOT/hexane/water microemulsions with different water concentrations ([AOT] = 1.12 M at 30.24% water).

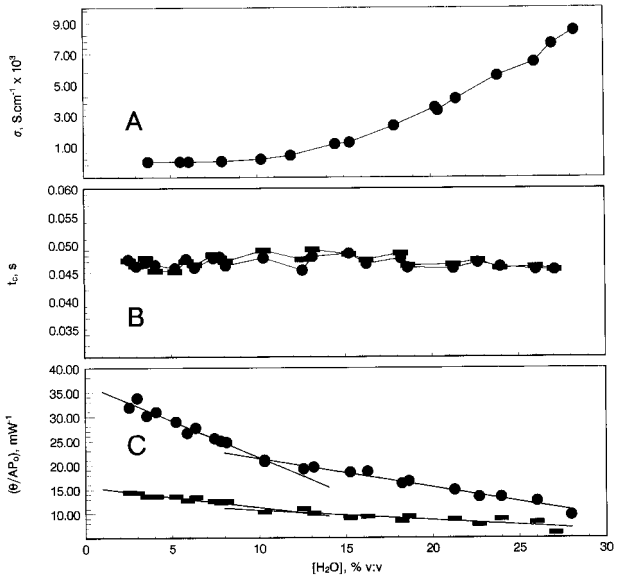

Figure 5. (A) Electrical conductivity, (B) t_c at 975 (●) and 872 nm (■), and (C) θ/AP_0 at 975 (●) and 872 nm (■) as a function of water percentage of the DDBABr/Cl−benzene/water microemulsion ([DDBABr] = 1.00 M at 27.08% water).

percolation threshold fell into the same straight line as the values measured below the percolation threshold for both wavelengths. The slope of the curve "θ/AP_0 versus water percentage" at 975 nm calculated using all the experimental points is 0.71 ± 0.02 mW^{-1} $\%^{-1}$. The slope calculated from samples that have water concentrations higher than 25.5% (from 25.7 to 31%) was 0.71 ± 0.09 mW^{-1} $\%^{-1}$, which is the same, within the experimental errors, as the slope calculated from points below the percolation threshold (i.e., 25.7−6.0%, slope = 0.76 ± 0.04 mW^{-1} $\%^{-1}$). Therefore, the variation of θ/AP_0 as a function of water percentage is the same below or above the percolation threshold. This result is similar to that observed for the microemulsion in $CF_2ClCFCl_2$.

The investigation was then continued with a positive surfactant (dodecyldimethylbutylammonium bromide, DDBABr). The electrical conductivity of this cationic emulsion is shown in Figure 5A. As illustrated, the electrical conductivity increases by almost 4 orders of magnitude concomitantly with the increase in the concentration of the dispersed phase. Furthermore, the increase in the electrical conductivity for this microemulsion is much larger than the increase observed for the AOT micro-

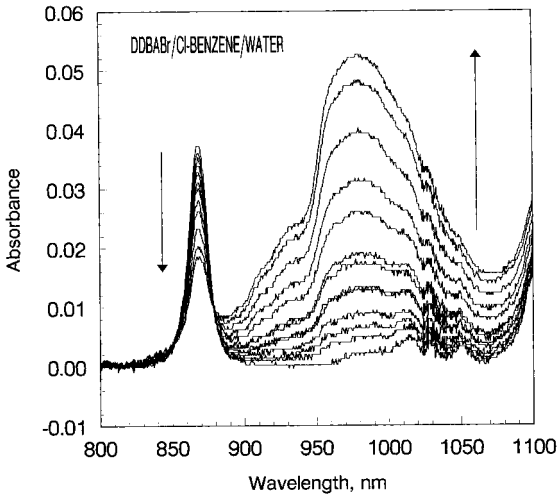

Figure 6. Near-IR absorption spectra of the DDBABr/Cl−benzene/water microemulsions with different water concentrations. Water concentrations (from bottom to top at 975 nm) were 0.00, 2.50, 2.87, 3.50, 4.50, 5.98, 9.22, 12.47, 15.13, 19.23, 20.00, 23.53, and 26.00%; [DDBABr] = 0.96 M at 26.00% water.

emulsions (see Figures 1A and 3A). Note that the electrical conductivity starts to increase at around 10% water, a value which is much smaller than the value of 27.5 and 26% observed for the AOT (Figures 1A and 3A, respectively). Note also that the increase in electrical conductivity is smoother than that observed for AOT. It is particularly interesting to observe such a different behavior between microemulsions prepared with AOT and DDBABr, considering that in both cases the W_0 value is the same. It may be argued that the differences observed are due solely to the differences in the electrical conductivity of the counterions of the surfactants. The ionic conductance of bromide ion (λ = 78.1 S cm^2 mol^{-1}) is, in fact, higher than that of sodium ion (λ = 50.1 S cm^2 mol^{-1}).[38] However, this difference is rather small to account for the much lower percolation threshold and the much larger magnitude of electrical conductivity observed for the DDBABr microemulsions (compared to AOT microemulsions). These effects are probably related to differences in the structure of the water−oil interfaces of these two microemulsions.

Figure 6 shows the near-IR absorption spectra of the DDBABr/Cl−benzene/water microemulsions, prepared at a constant W_0 value of 15 and at different water concentrations. Two absorption peaks (975 and 869 nm) and a shoulder at 935 nm can be visualized. They can be attributed to water and chlorobenzene, and to the surfactant, respectively. Increasing water concentration leads to an increase in the water's and surfactant's peaks and a decrease in the chlorobenzene's peak. The thermal lens signals were measured at 975 and 872 nm in order to obtain information on the aqueous and the oil phases, respectively.

Figure 5B shows t_c values at 975 and 872 nm measured as a function of water concentration. It is clear from the figure that there is almost no change in the t_c value as a function of the water percentage. The k value of chlorobenzene is smaller than k of water (Table 2). It is expected, consequently, that t_c should increase concomitantly with the increase in the concentration of chlorobenzene. The lack of variation in the t_c value can be explained by the variations in k, ρ, and c_p. In this case the decrease in k value must be adequately compensated for by the decrease in the values of ρ and c_p (eq 5).

Figure 5C shows the variation of θ/AP_0 as a function of water concentration measured at 975 and 872 nm. For both wavelengths the curves do not have the same slopes for the whole

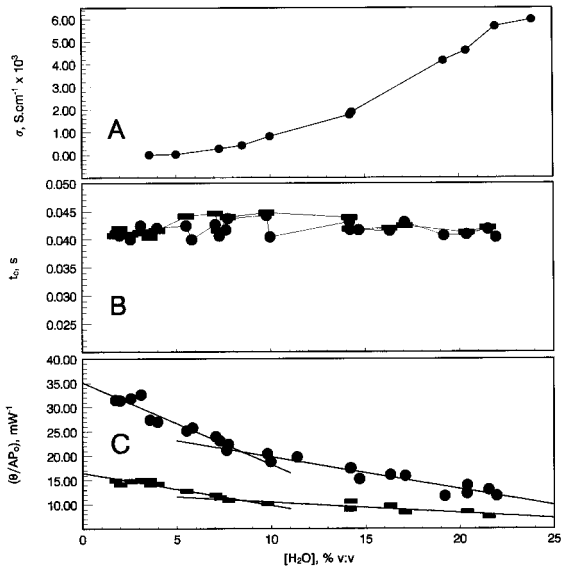

Figure 7. (A) Electrical conductivity, (B) t_c at 975 (●) and 872 nm (■), and (C) θ/AP_0 at 975 (●) and 872 nm (■) as a function of water percentage for the BDHACl/benzene/water microemulsion ([BDHACl] = 0.73 M at 21.95% water).

concentration range monitored. In fact, at around 10% water (concentration above which the electrical conductivity starts to increase) there is a change in the slope. For 975 nm the slope measured for concentrations equal and above 10% water was calculated to be 0.59 ± 0.03 mW^{-1} %$^{-1}$. For the concentrations equal and below 10% water it was calculated to be 1.5 ± 0.1 mW^{-1} %$^{-1}$. For 872 nm, the slope calculated using the concentrations equal and above 10% water was 0.20 ± 0.04 mW^{-1} %$^{-1}$ and 0.43 ± 0.06 mW^{-1} %$^{-1}$ for concentrations equal and lower than 10% water. Clearly, for both wavelengths, there is a pronounced change in the slope of θ/AP_0 as a function of water percentage, and the change in the slope seems to occur at the same concentration range where the electrical conductivity of the microemulsion starts to change. This variation in the slope is interesting and may be correlated with the variation in the internal structure of the system.

Shown in Figure 7A is the electrical conductivity of microemulsions prepared using another positively charged surfactant, benzyldimethyl-*n*-hexadecylammonium chloride, in benzene, plotted as a function of water concentration (at a constant $W_0 = 16$). Note that, with the increase in the concentration of the dispersed phase, there is an increase in the electrical conductivity of almost 4 orders of magnitude, starting at around 9% water. Also, in this case the increase in electrical conductivity is much smoother than that observed for AOT.

The near-IR absorption spectra of these microemulsions for several water concentrations (and at a constant W_0 of 16) are shown in Figure 8. The peak at 975 nm is due to water, and the peak at 872 nm is due to the C−H groups of the benzene rings in the oil phase as well as in the surfactant. The shoulder at 935 nm is due to the absorption of the aliphatic C−H groups of the surfactant.[31] Accordingly, the thermal lens measurements were performed at 872 and 975 nm.

As can be seem from Figure 7B, t_c measured at 975 and 872 nm is almost constant for the whole concentration range. This seems to suggest that t_c is insensitive to any changes in the internal structure of the microemulsion. Conversely, θ/AP_0 increases with the decrease in the micellar phase concentration (Figure 7C). It is clear from the figure that there is a change in the slope of θ/AP_0 as a function of water concentration at around 9% water. The slope measured at 975 nm, calculated using the experimental points with water concentrations higher than

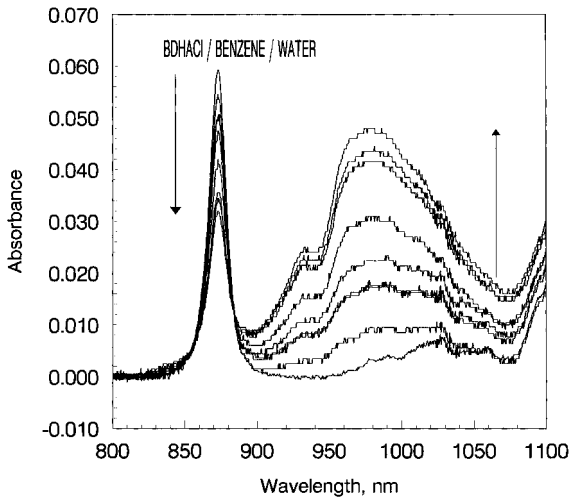

Figure 8. Near-IR absorption spectra of the BDHACl/benzene/water microemulsions with different water concentrations. Concentrations of water (from bottom to top at 975 nm) were 0.00, 3.58, 7.28, 7.48, 9.98, 14.21, 19.19, 20.39, and 21.95% ([BDHACl] = 0.73 M at 21.95% water).

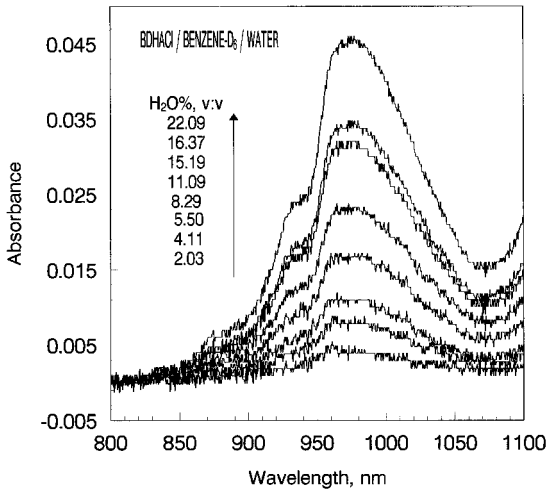

Figure 9. Near-IR absorption spectra of the BDHACl/benzene-d_6/water microemulsions with different water concentrations ([BDHACl] = 0.73 M at 22.09% water).

9%, is 0.66 ± 0.07 mW^{-1} %$^{-1}$ and using the points with water concentrations lower than 9% is 1.7 ± 0.2 mW^{-1} %$^{-1}$. At 872 nm the slope calculated using the points with concentrations higher than 9% is 0.22 ± 0.05 mW^{-1} %$^{-1}$ and is 0.67 ± 0.08 mW^{-1} %$^{-1}$ using the points with concentrations lower than 9%. Similar to the effect observed for the DDBABr/Cl−benzene/water microemulsion, it is evident that for both wavelengths there is a change in the slope of θ/AP_0 versus water concentration, and the change seems to occur at the same concentration range where the electrical conductivity of the microemulsion starts to increase.

In the BDHACl/benzene/water microemulsion, both the solvent and the surfactant absorb at 872 nm. To obtain more detailed information on the observed effect, similar measurements were performed with the microemulsion prepared with the same surfactant but with deuterated benzene (i.e., BDHACl/benzene-d_6/water). In this case, only the C−H groups of the surfactant is excited at 872 nm. The near-IR absorptions of these microemulsions are shown in Figure 9. As in the BDHACl/benzene/water microemulsions, the peak at 975 nm is due to water, the small peak at 872 nm is due to the benzene ring of the surfactant, and the shoulder at 935 nm is due to

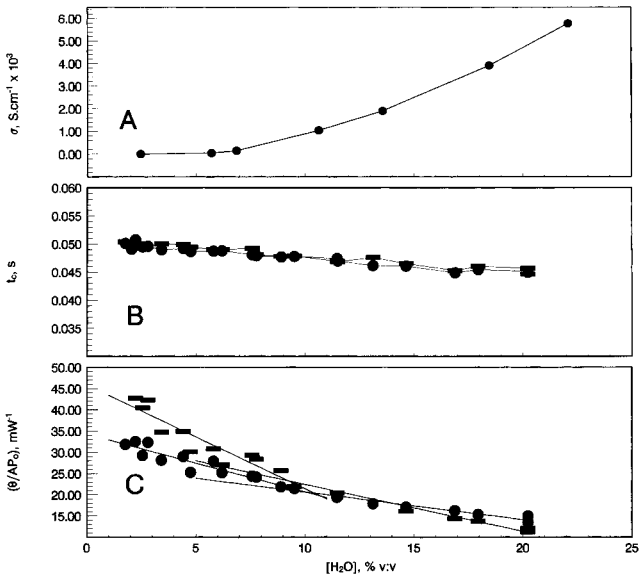

Figure 10. (A) Electrical conductivity, (B) t_c at 975 (●) and 872 nm (■), and (C) θ/AP_0 at 975 (●) and 872 nm (■) as a function of water percentage of the BDHACl/benzene-d_6/water microemulsion ([BDHACl] = 0.73 M at 21.95% water).

aliphatic C−H absorption from the surfactant. The thermal lens measurements were also performed at 872 and 975 nm.

Figure 10A shows the electrical conductivity for the BDHACl/benzene-d_6/water microemulsion as a function of water concentration. Note that, with the increase in the concentration of the dispersed phase, there is an increase in the electrical conductivity of almost 4 orders of magnitude. Similar to the DBABr/Cl−benzene/water and BDHACl/benzene/water microemulsions, the electrical conductivity starts to increase at around 9% water. Again, this value is much smaller than the values for the AOT (27.5% in Figure 1A and 26% in Figure 3A). Also, the increase in electrical conductivity is smoother than that observed with AOT. As can be seem from Figure 10B, t_c values, measured at 975 and 872 nm, exhibit only a small decreasing variation as a function of water concentration. There was not, however, any evidence of changes in the slope of the "t_c versus [water]" curve in the whole concentration range studied.

Conversely, the value of θ/AP_0 increases with the decrease in the micellar phase concentration (Figure 10C). There is a change in the slope of θ/AP_0 as a function of water percentage at around 9% water. The slope calculated using the experimental points with concentration higher than 9% (measured at 975 nm) is 0.65 ± 0.04 mW^{-1} %$^{-1}$, and using the points with concentration lower than 9% is 1.35 ± 0.2 mW^{-1} %$^{-1}$. At 872 nm the slopes are 1.1 ± 0.1 and 2.4 ± 0.4 mW^{-1} %$^{-1}$ for concentrations higher and lower than 9%, respectively. Similar to the effect observed for the other microemulsions prepared with positively charged surfactants, it is evident that for both wavelengths there is a change in the slope of θ/AP_0 as a function of water percentage, and the change in the slope seems to occur at the same concentration range where the electrical conductivity of the microemulsion starts to increase.

Discussion

The refractive index is known to be sensitive to changes in the structure and/or phase of microemulsions.[39,40] It is expected, therefore, that dn/dT should also be sensitive to structural changes and to the thermal lens signal intensity (eq 4). In fact, the thermal lens technique has been used to study the effect of nonelectrolytes and surfactants on the structure of water[19] and the mechanism of the differences in the anisotropic heat conductivity and the dn/dT values of different liquid crystals.[41,42] It is expected, therefore that by analyzing the parameter θ/AP_0, which is proportional to dn/dT, insight into the internal structure of the investigated systems can be obtained. The other parameter investigated, i.e. t_c, was shown to be insensitive to any structural change of the microemulsions. Rather, it was evident from the data shown in Figures 1B, 2B, 5B, 7B, and 10B that t_c has either none or only a minor linear variation with water percentage below and above the percolation threshold.

Two interesting aspects were observed for both microemulsions prepared with the negatively charged surfactant (AOT/$CF_2ClCFCl_2$/water, AOT/hexane/water): namely, the increase in electrical conductivity was observed only at relatively high dispersed phase concentrations (above 26% water), and the same linear relationship between θ/AP_0 and the water concentration was observed above and below the percolation threshold. The fact that the thermal lens signal has the same slope as a function of water concentration suggests that there is probably no change in the structure of the microemulsions above or below the percolation threshold. This would also explain the observation that the electrical conductivity increases only at relatively high concentration of the micellar phase. Because the size of the structures in solution did not increase with the concentration of the dispersed phase, it is necessary to have high micellar concentration in order for the electrical charges to be conducted through macroscopic distances (by ion hopping or fast material exchange when the droplets coalesce). In fact, at 26% water the volume fraction of the dispersed phase is equal to 64 and 70% for the AOT microemulsions prepared with hexane and $CF_2ClCFCl_2$, respectively. These values are compared with the hard-sphere close-packing limit volume fraction (65%).[3] This lack of variation of micellar structure with the increase in the concentration of dispersed phase can be explained by the characteristics of the AOT films at these low W_0 values (and in the absence of salt). The AOT tend to form rigid interfaces with high curvature, and as a consequence, the attractive forces between micelles are rather small (for the case of $W_0 = 15$).[3] Therefore, the reversed micelles do not have a tendency to form lower curvature structures or to have their size increased concomitantly with the concentration of the dispersed phase. It is known that at the low dispersed phase concentration region the (water in oil) microemulsions of AOT with W_0 equal to 15 are constituted of reversed micelles with hydrodynamic radius equal to 40 Å (isooctane).[43] It is also estimated that there are 45−65 monomers per reversed micelle (cyclohexane).[44] The present results suggest that above the percolation threshold the same structure is still present. This is in agreement with previous works based on FT-IR,[26] refractive index,[6] small-angle neutron diffraction,[28,45] and photon correlation spectroscopy.[43]

For the microemulsions prepared with the positively charged surfactants (DDBABr/Cl−benzene/water, BDHACl/benzene/water, BDHACl/benzene-d_6/water) two interesting effects were observed in all systems investigated: namely, the increase in electrical conductivity was observed at relatively low dispersed phase concentration (around 10% water, that is equal to 22, 25, and 24% of volume fraction of dispersed phase for the DDBABr/Cl−benzene/water, BDHACl/benzene/water, BDHACl/benzene-d_6/water microemulsions, respectively), and the observed change in the slope of the θ/AP_0 as a function of water concentration at the same region where the electrical conductivity changes. The change in the slope seems to indicate that there is a change in the internal structure of the microemulsions. It is probably related to the increase in the size of the reversed micelles with the concentration of the dispersed phase. This eventually leads

to the formation of bicontinuous structures in solution. In other words, at the high dispersed phase concentration region, where larger aggregates are present, the changes in the θ/AP_0 of the microemulsion as a function of the concentration of micelles are different from the changes at low concentration where the microemulsion consists of relatively small reversed micelles. The fact that the change in the slope is in the same concentration range as the change in the electrical conductivity provides further support for the explanation that the change in structure of the microemulsion is related to the percolation phenomenon.

The aggregation of micelles which eventually leads to the formation of bicontinuous structures in solution can be used to explain the relatively low percolation threshold value. With the increase in the concentration of the dispersed phase there is an increase in the number of conducting water channels and, as a consequence, an increase in the electrical conductivity. This explains the relatively smooth variation of σ as a function of water percentage. The propensity to form larger structures in solution can be explained by the high fluidity and the tendency to form low-curvature films of the positively charged surfactants studied. This would result in large attractive values for the intermicellar interaction, as has been measured by Zana et al.[5,53] This proposed picture is in agreement with self-diffusion and conductivity experiments performed by Chatenay et al.[46] Zana et al.[31] using fluorescence quenching experiments concluded that in both DDBABr/Cl−benzene/water and DBHACl/benzene/water microemulsions the percolation phenomenon could still be explained by the coalescence of aggregates and fast material exchange. However, the same authors concluded that with longer time scale techniques (self-diffusion ^{1}H NMR and conductivity experiments) these microemulsions exhibit characteristics of bicontinuous phases.[31] This apparent contradiction can probably be explained by the dynamic behavior and the lack of long-range order of these phases. In the present study, the thermal lens signals were usually measured over a period that corresponds to 3−4 times the thermal time constant t_c (i.e., about 0.2−0.4 s), which is on a time scale similar to that of the self-diffusion ^{1}H NMR. The results obtained agree with the formation of larger interconnected aggregates or bicontinuous structures in solution.

It is known that percolation is a phase transition-like phenomenon where an interconnected random structure is formed which spans the entire system and may be governed by universal scaling law. The validity of such law for the microemulsions used in this study (BDHACl/benzene/water, DDBABr/Cl−benzene/water, and AOT/trichlorotrifluoroethane/water) was evaluated. According to the most widely used theoretical model, which is based on the dynamic nature of the microemulsions,[47−49] there are two pseudophases: one in which the charge is transported by the diffusion of the microemulsion globules (reversed micelles) and the other phase in which the charge is conducted by diffusion of the charge carrier itself inside the reversed micelle clusters. According to this theory

$$\sigma = (\phi - \phi_c)^t \qquad \text{for } \phi > \phi_c \tag{6}$$

$$\sigma/\phi = (\phi_c - \phi)^{-s} \qquad \text{for } \phi < \phi_c \tag{7}$$

where σ is the electrical conductivity, ϕ is the water volume fraction, and ϕ_c is the critical water volume fraction of the conducting phase (percolation threshold).[50]

According to these equations, for $\phi > \phi_c$, the plot of log σ versus log($\phi - \phi_c$) should give a slope equal to t. For $\phi < \phi_c$ it is necessary to correct for the intrinsic conductivity of microemulsions before the percolation threshold, and the plot

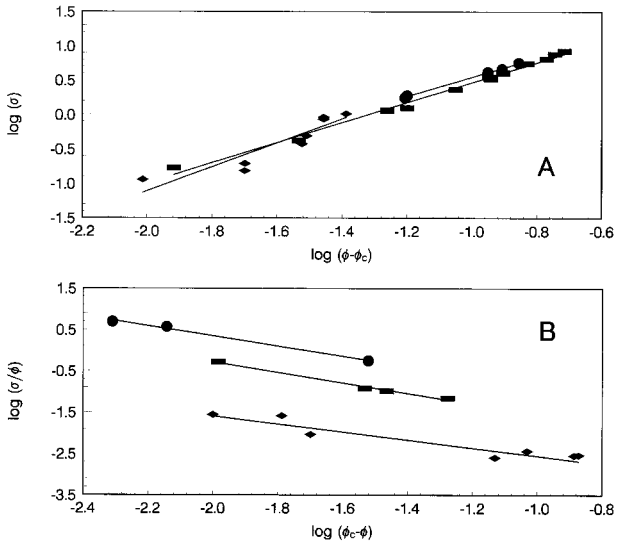

Figure 11. Plots of (A) log σ vs log ($\phi - \phi_c$) for $\phi > \phi_c$ and (B) log (σ/ϕ) vs log ($\phi - \phi_c$) for $\phi < \phi_c$ for (◆) AOT/$CF_2ClCFCl_2$/water, (■) DDBABr/Cl-benzene/water, and (●) BDHACl/benzene/water microemulsions whose ϕ_c values are 0.27, 0.09, and 0.08, respectively.

TABLE 3: Exponents of the Variation of Electrical Conductivity (σ) as a Function of Water Volume Fraction (ϕ)

microemulsion system	t	s
AOT/trichlorotrifluoroethane/water	1.7 ± 0.3	1.0 ± 0.2
BDHACl/benzene/water	1.40 ± 0.05	1.2 ± 0.1
DDBABr/Cl−benzene/water	1.46 ± 0.05	1.3 ± 0.1

of log of specific conductivity (σ/ϕ) as a function of log($\phi_c - \phi$) should provide the value for s.[50] Such plots for the three microemulsion systems are shown in Figure 11. The t and s values obtained from the plots are listed in Table 3.

The theoretical model for the percolation in static systems predicts that the exponents t and s should be 1.6 and 0.7, respectively.[51−53] However, because of the dynamic nature of the microemulsions, it has been theoretically and experimentally shown that both exponents should be higher than those predicted for the static case.[47−49,54,55] Most of the s values reported for microemulsions are around 1.2, which is in good agreement with the 1.0, 1.2, and 1.3 values obtained in this study.[47−49,54,55] The values of t are more scattered. It was reported to be anywhere from 1.4 to 2.0, with 1.6 being the value which is most often found.[50,56] The values of t found in this studies are also in the 1.4−2.0 range. However, the t values for the positively charged surfactants are somewhat in the lower part of this range (1.40 and 1.46). The formation of the bicontinuous structure in the solution of the cationic microemulsions is probably the reason for this deviation.

Conclusion

It is possible to deduce internal structural information for microemulsion systems above and below the percolation threshold by use of the described near-IR absorption and thermal lens techniques, together with the electrical conductivity measurements. The change in the slope of θ/AP_0 as a function of the dispersed phase concentration is correlated with the changes in the internal structure of the microemulsions.

For the negatively charged AOT microemulsions, the lack of variation in the slope of "θ/AP_0 versus water percentage" curve and the high concentration percolation threshold are probably due to the fact that these microemulsions are constituted of reversed micelles whose sizes are similar and independent of the concentration of dispersed phase.

For the microemulsions prepared with the positively charged surfactants DBHACl and DDBABr, the change in the slope of θ/AP_0 as a function of the dispersed phase concentration occurs at same concentration range where the electrical conductivity undergoes changes. This, together with the observed low percolation threshold concentration, can be interpreted as due to the change in the structure of the microemulsion concomitantly with the increase in the concentration of dispersed phase. It is proposed that the size of the reversed micelles grow to eventually form highly interconnected aggregates or bicontinuous structures in solution.

Acknowledgment. The authors are grateful to the National Institutes of Health for financial support of this work.

References and Notes

(1) Chen, S.-H., Rajagopalan, R., Eds. In *Micellar Solutions and Microemulsions*; Springer-Verlag: New York, 1990.
(2) Friberg, S. E., Bothorel, P., Eds. In *Microemulsions: Structure and Dynamics*; CRC Press: Boca Raton, FL, 1987.
(3) Alexandridis, P.; Holzwarth, J. F.; Hatton, T. A. *J. Phys. Chem.* **1995**, *99*, 8222.
(4) Grest, G. S.; Webman, I.; Safran, S. A.; Bug, A. L. R. *Phys. Rev. A* **1986**, *33*, 2842.
(5) Jada, A.; Lang, J.; Zana, R.; Makhloufi, R.; Hirsch, E.; Candau, S. J. *J. Phys. Chem.* **1990**, *94*, 387.
(6) Goffredi, M.; Liveri, V. T.; Vassalo, G. *J. Solution Chem.* **1993**, *22*, 941.
(7) Scriven, L. E. *Nature* **1976**, *263*, 123.
(8) Clausse, M.; Peyrelasse, J.; Heil, J.; Boned, C.; Lagourette, B. *Nature* **1981**, *293*, 636.
(9) Borkovec, M.; Eicke, H.-F.; Hammericli, H.; Das Gupta, B. *J. Phys. Chem.* **1988**, *92*, 206.
(10) Datema, K. P.; Bolt-Westerhoff, J. A.; Jaspers, A.; Daane, J. G. R.; Rupert, L. A. M. *Magn. Reson. Chem.* **1992**, *30*, 760.
(11) Vollmer, D.; Vollmer, J.; Eicke, H.-F. *Europhys. Lett.* **1994**, *26*, 389.
(12) Lindman, B.; Shinoda, K.; Olsson, U.; Anderson, D.; Karlström, G.; Wennerström, H. *Colloids Surf.* **1989**, *38*, 205.
(13) Sánchez-Rubio, M.; Santos-Vidals, L. M.; Rushforth, D. S.; Puig, J. E. *J. Phys. Chem.* **1985**, *89*, 411.
(14) Williams, P., Norris, K., Eds. In *Near-Infrared Technology in the Agricultural and Food Industries*; American Association of Cereal Chemists: St. Paul, Mn, 1987.
(15) Burns, D. A.; Ciurczak, E. W. In *Handbook of Near-Infrared Analysis*; Marcel Dekker: New York, 1992.
(16) Tran, C. D.; Grishko, V. I.; Baptista, M. S. *Appl. Spectrosc.* **1994**, *48*, 833.
(17) Tran, C. D. In *Photoacoustic and Photothermal Phenomena III*; Bicanic, D., Ed.; Springer-Verlag: Berlin, 1992; pp 463−473.
(18) Tran, C. D. *Anal. Chem.* **1988**, *60*, 182.
(19) Baptista, M. S.; Tran, C. D. *J. Phys. Chem.* **1995**, *99*, 12952.
(20) Franko, M.; Tran, C. D. *J. Phys. Chem.* **1991**, *95*, 6688.
(21) Thorne, J. B.; Bobbitt, D. R. *Appl. Spectrosc.* **1993**, *47*, 360.
(22) Tran, C. D. In HPLC Detection: Newer Methods; Patonay, G., Ed.; VCH: New York, 1992; Chapter 6, pp 111−126.
(23) Vyas, R.; Gupta, R. *Appl. Opt.* **1988**, *27*, 4701.
(24) Scheldon, S. J.; Knight, L. V.; Thorne, J. M. *Appl. Opt.* **1982**, *21*, 1663.
(25) Carter, C. A.; Harris, J. M. *Appl. Opt.* **1984**, *23*, 476.
(26) (a) Giammona, G.; Goffredi, F.; Liveri, T. V.; Vassalo, G. *J. Colloid Interface Sci.* **1992**, *154*, 411−415. (b) Goffredi, F.; Liveri, V. T.; Vassallo, G. *J. Colloid Interface Sci.* **1992**, *151*, 396−401.
(27) D'Aprano, A.; D'Arrigo, G.; Paparelli, A.; Goffredi, M.; Liveri, V. T. *J. Phys. Chem.* **1993**, *97*, 3614−3618.
(28) Kotlarchyk, M.; Chen, S. H.; Huang, J. S.; Kim, M. W. *Phys. Rev. Lett.* **1984**, *53*, 941−944.
(29) Chen, S. H.; Huang, J. S. *Phys. Rev. Lett.* **1985**, *55*, 1888−1891.
(30) Cazabat, A. M.; Chatenay, D.; Guering, P.; Urbach, W.; Langevin, D.; Meunier, J. In *Microemulsion Systems*; Rosano, H. L., Clausse, M., Eds.; Marcel Dekker: New York, 1987; pp 183−198.
(31) Zana, R.; Lang, J.; Canet, D. *J. Phys. Chem.* **1991**, *95*, 3364−3367.
(32) Weyer, L. G. *Appl. Spectrosc. Rev.* **1985**, *21*, 1.
(33) Dovichi, N. J. *CRC Crit. Rev. Anal. Chem.* **1987**, *17*, 357.
(34) Riddick, J. A.; Bunger, W. B.; Sakano, T. K. *Organic Solvents Physical Properties and Methods of Purification*, 4th ed.; Wiley: New York, 1986; Vol. 2.
(35) Radlińska, E. Z.; Hyde, S. T.; Ninham, B. W. *Langmuir* **1989**, *5*, 1427.
(36) Ray, S.; Bisal, S. R.; Moulik, S. P. *Langmuir* **1994**, *10*, 2507.
(37) Moulik, S. P.; Das, M. L.; Bhattacharya, P. K.; Das, A. R. *Langmuir* **1992**, *8*, 2135.
(38) Atkins, P. W. In *Physical Chemistry*, 4th ed.; Freeman: New York, 1990; p 752.
(39) Clausse, M.; Zradba, A.; Heil, J.; Rouviere, J.; Sohounhloue, K. In *Microemulsion Systems*; Rosano, H. L., Clausse, M., Eds.; Dekker: New York, 1987.
(40) Rebbouh, N.; Buchert, J.; Lalanne, J. R. *Europhys. Lett.* **1987**, *4*, 447.
(41) Fuh, Y. G.; Code, R. F. *Can. J. Phys.* **1984**, *63*, 282.
(42) Ono, H.; Kazuhiko, T.; Fujiwara, K. *Appl. Spectrosc.* **1995**, *49*, 1189.
(43) Zulauf, M.; Eicke, H.-F. *J. Phys. Chem.* **1979**, *83*, 480.
(44) Fendler, J. H. *Membrance Mimetic Chemistry*; Wiley: New York, 1982.
(45) Kotlarchyk, M.; Chen, S. H.; Huang, J. S. *J. Phys. Chem.* **1982**, *86*, 3273.
(46) Chateney, D.; Urbach, W.; Cazabat, A. M.; Langevin, D. *Phys. Rev. Lett.* **1985**, *54*, 2253.
(47) Lagues, M. *J. Phys. Lett.* **1979**, *40*, L331.
(48) Grest, G. S.; Webman, I.; Safran, S. A.; Bug, A. L. R. *Phys. Rev. A* **1986**, *33*, 2842−2845.
(49) Safran, S. A.; Grest, G. S.; Bug, A. L. R. In Percolation in Interacting Microemulsions; Rosano, H. L., Clausse, M., Eds.; Marcel Dekker: New York, 1987; pp 235−243.
(50) Laguës, M.; Sauterey, C. *J. Phys. Chem.* **1980**, *84*, 3503−3508.
(51) Webman, I.; Jortner, J. *Phys. Rev. B* **1977**, *16*, 2593−2596.
(52) Song, Y.; Noh, T. W.; Lee, S.-I.; Gaines, J. R. *Phys. Rev. B* **1986**, *33*, 904−908.
(53) Straley, J. P. *Phys. Rev. B* **1977**, *15*, 5733−5737.
(54) Peyrelasse, J.; Moha-Ouchane, M.; Boned, C. *Phys. Rev. A* **1988**, *38*, 4155−4161.
(55) Boned, C.; Peyrelasse, J.; Saidi, Z. *Phys. Rev. E 47*, 468−478.
(56) Mehta, S. K.; Bala, K. *Phys. Rev. E* **1995**, *51*, 5732−5737.